Biological Journal of the Linnean Society, 2006, **88**, 101–118. With 6 figures

The geography of diversification in the mormoopids (Chiroptera: Mormoopidae)

LILIANA M. DÁVALOS*

Department of Ecology, Evolution and Environmental Biology, Columbia University and Division of Vertebrate Zoology, American Museum of Natural History, Central Park West at 79th Street, New York, NY 10024-5192, USA

Received 22 October 2004; accepted for publication 1 July 2005

The traditional explanation of the distribution of the Mormoopidae is that this family originated in southern Central America or northern South America, later expanding its range north to Mexico and the West Indies, and differentiating into eight species. An alternative fossil-based hypothesis argues that the family originated in the northern Neotropics, reached the Caribbean early in its history, and dispersed to South America after the completion of the Isthmus of Panama. The present study analyses new and previously published sequence data from the mitochondrial 12S, $tRNA^{val}$, 16S, and cytochrome *b*, and the nuclear *Rag*2, to evaluate species boundaries and infer relationships among extant taxa. Fixed differences in cytochrome *b* often coincide with published morphological characters and show that the family contains at least 13 species. Two additional, morphologically indistinct, lineages are restricted to Suriname and French Guiana. Phylogeny-based inferences of ancestral area are equivocal on the geographical origin of mormoopids, in part because several internal nodes are not resolved with the available data. Divergences between Middle American and Antillean populations are greater than those between Mexico/Central America and South America. This suggests that mormoopids diversified in northern Neotropics before entering South America. A northern neotropical origin for mormoopids is congruent with both the Tertiary fossil record and recent phylogenetic hypotheses for the sister family to the Mormoopidae, the Phyllostomidae.

ADDITIONAL KEYWORDS: dispersal-vicariance analysis – *Mormoops* – Phyllostomidae – *Pteronotus* – *Pteronotus fulvus* – *Pteronotus psilotis* – *Pteronotus pusillus* – *Pteronotus portoricensis* – *Pteronotus rubiginosus*.

INTRODUCTION

The Mormoopidae is a neotropical family of bats characterized by flap-like outgrowths of skin below the lower lip and funnel-shaped ears (Simmons & Conway, 2001). The two extant genera, *Mormoops* and *Pteronotus*, range from Texas south through Mexico, Central America, the West Indies, and through northern South America to the Mato Grosso of Brazil, and west of the Andes to Peru (Koopman, 1994). Geographic variation within all but two of the extant species, *Mormoops blainvillei* and *Pteronotus gymnonotus*, is recognized by partition into more than 20 subspecies (Table 1).

*Current address: Department of Biochemistry and Molecular Biophysics, 208 Life Sciences South, University of Arizona, Tucson, AZ 85721, USA. E-mail: davalos@amnh.org

Interest in the phylogeny of the Mormoopidae has flourished recently, with morphological (Simmons & Conway, 2001), molecular (Lewis Oritt, Porter & Baker, 2001; Van Den Bussche & Weyandt, 2003), and combined analyses (Van Den Bussche, Hoofer & Simmons, 2002b) published in rapid succession. These different sources of data have independently supported the monophyly of mormoopids, and of both *Mormoops* and *Pteronotus* (Lewis Oritt *et al*., 2001; Simmons & Conway, 2001; Van Den Bussche *et al*., 2002b). At the same time, the phylogenetic relationships of mormoopids to other chiropteran families is now better understood than ever before. Mormoopidae is sister to Phyllostomidae (Van Den Bussche & Hoofer, 2000; Simmons & Conway, 2001; Teeling, Madsen, Murphy, Springer & O'Brien, 2003), and closely allied with the New World family Noctilionidae and the New Zealand

Table 1. Currently recognized taxa, geographical distribution, and molecular sequences included in this study

Species	Subspecies	Distribution	DNA sequences available
Mormoops magna†		Cuba (Quaternary)	
Mormoops blainvillei		Greater Antilles †Bahamas Gonave Antigua Barbuda	*Rag2* 12S $tRNA^{val}$ 16S cyt *b* = 3
Mormoops megalophylla	*megalophylla*	Texas to Nicaragua †Greater Antilles Bahamas	*Rag2* 12S $tRNA^{val}$ 16S cyt *b* = 4
Mormoops megalophylla	*tumidiceps*	Colombia Venezuela Trinidad Margarita	cyt *b* 12S $tRNA^{val}$ 16S
Mormoops megalophylla	*intermedia*	Aruba Bonaire Curacao	
Mormoops megalophylla	*carteri*	Ecuador NW Peru	
Pteronotus sp.†	cf. *rubiginosus*	Hispaniola (Quaternary)	
Pteronotus parnellii	*parnellii*	Cuba Jamaica	*Rag2* cyt *b* = 3
Pteronotus pristinus†		Cuba Florida (Quaternary)	
Pteronotus parnellii	*pusillus*	Hispaniola †Gonave	cyt *b* = 2
Pteronotus parnellii	*portoricensis*	Puerto Rico	cyt *b* = 2
Pteronotus parnellii	*mexicanus*	Mexico excluding Veracruz and Yucatán	cyt *b* = 2
Pteronotus parnellii	*mesoamericanus*	SE Veracruz to SW Panama	cyt *b* = 2
Pteronotus parnellii	*rubiginosus*	Honduras to no. South America Trinidad Tobago	12S $tRNA^{val}$ 16S cyt *b* = 4
Pteronotus parnellii	*fuscus*	NE Colombia NW Venezuela	
Pteronotus parnellii	*paraguanensis*	Paraguaná	
Pteronotus personatus	*personatus*	Nicaragua to South America	*Rag2* cyt *b* = 3
Pteronotus personatus	*psilotis*	Mexico to Honduras	12S $tRNA^{val}$ 16S cyt *b* = 2
Pteronotus macleayii	*macleayii*	Cuba †Bahamas	*Rag2* 12S $tRNA_{val}$ 16S cyt *b*
Pteronotus macleayii	*griseus*	Jamaica	cyt *b* = 2
Pteronotus quadridens	*quadridens*	Cuba †Bahamas	*Rag2* 12S $tRNA^{val}$ 16S cyt *b*
Pteronotus quadridens	*fuliginosus*	Greater Antilles excluding Cuba	cyt *b* = 4
Pteronotus davyi	*davyi*	Nicaragua to Venezuela Trinidad Dominica Martinique	*Rag2* = 3 12S $tRNA^{val}$ 16S cyt *b* = 4
Pteronotus davyi	*fulvus*	Mexico to Honduras	cyt *b* = 3
Pteronotus davyi	*incae*	Peru	
Pteronotus gymnonotus		Veracruz to French Guiana and Brazil	*Rag2* 12S $tRNA^{val}$ 16S cyt *b* = 3

Most molecular data were obtained from previous studies: 12S rRNA, $tRNA^{val}$, 16S rRNA from Van Den Bussche & Hoofer (2000) and Van Den Bussche *et al*. (2002b), cytochrome *b* and *Rag*2 from Lewis Oritt *et al*. (2001). See 'Taxon sampling' for cytochrome *b* (cyt *b*) sequences generated in this study, and the Appendix for GenBank accession numbers. †Extinct taxon (i.e. population, unavailable for molecular analyses). When several sequences were used, = *n* indicates the number of sequences available.

Short-tailed bat *Mystacina tuberculata* (Mystacinidae) in the noctilionoid clade (Kennedy *et al.*, 1999; Pierson *et al.*, 1986; Kirsch *et al.*, 1998; Van Den Bussche & Hoofer, 2000).

Two hypotheses explain the diversification of this family in relation to its geographical distribution. Smith (1972) proposed that the mormoopids originated in southern Central America or north-western South America, reaching the Caribbean through repeated dispersal from Mexico and/or Central America (Fig. 1). Three predictions stem from his biogeographical hypothesis: (1) southern Central America and/or north-western South America will be part of the ancestral area of the family; (2) the closest relative of each of the Caribbean mormoopid lineages will range into Mexico and/or Central America; and (3) the ages of divergence between Antillean mormoopids and their continental relatives will be *Pteronotus quadridens* and *Pteronotus macleayii* > *M. blainvillei* > *Pteronotus parnellii* (Fig. 1). By contrast, and based mostly on the fossil record, Czaplewski & Morgan (2003) hypothesized that mormoopids expanded their range to the Greater Antilles early in their history, reaching South America only after the completion of the Panama land bridge in the Pliocene. Therefore, the ancestral area of mormoopids will not include north-western South America and might include the Greater Antilles, and the divergences between Antillean and continental lineages will be older than those between Central

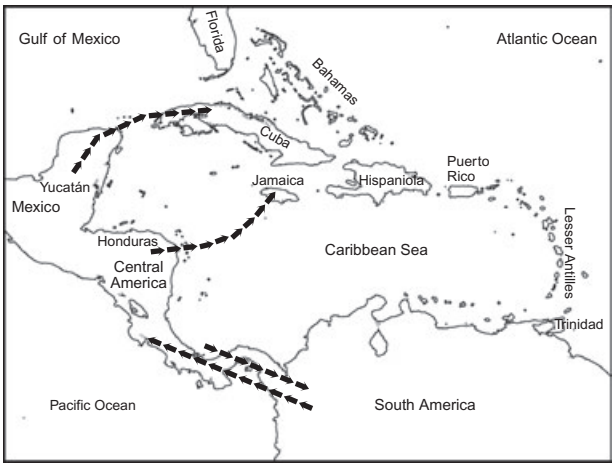

Figure 1. Map of the Caribbean and biogeographical hypotheses about the origin of mormoopids. According to Smith (1972), ancestral mormoopids dispersed from northern South America or southern Central America to Mexico/Central America. From there, the ancestors of Greater Antillean mormoopids reached the West Indies through Cuba via Yucatán, or Jamaica via Honduras. Dispersal through these routes would explain the distribution of the single lineage comprising *Pteronotus quadridens* and *macleayii* (ancient), the species *Mormoops blainvillei* (less ancient), and the Caribbean populations of *Pteronotus parnellii* (most recent). Czaplewski & Morgan (2003) concur on the dispersal routes to the Caribbean, but propose that mormoopids colonized the islands early in their evolutionary history. From Mexico/Central America, mormoopids would have reached South America recently, after the closing of the Isthmus of Panama.

American and northern South American mormoopid populations.

The present study aimed to evaluate the two competing biogeographical hypotheses in light of the recent progress toward resolving phylogenetic relationships among extant mormoopids. An assessment of evolutionary independence among mormoopid populations currently considered conspecific was crucial. New and published mitochondrial cytochrome *b* (1.14 kb) sequences were used to clarify this question. These sequences and published morphological and nuclear *Recombination activating gene* 2 (*Rag*2) data were analysed to estimate phylogenies for the family. The resulting phylogenies were used to evaluate the predictions of the hypotheses of Smith (1972) and Czaplewski & Morgan (2003).

MATERIAL AND METHODS

TAXON SAMPLING

To examine relationships among the mormoopids, both genera and 18 of the 22 currently recognized subspecies were included in the study (Simmons, 2005). A list of taxa with sequences analysed is shown in Table 1, and the complete GenBank numbers and vouchers are listed in the Appendix. Most cytochrome *b* sequences (1.14 kb), and all mitochondrial 12S, $tRNA^{val}$, 16S genes (the last three hereafter referred to as mitochondrial ribosomal DNA or mtrDNA, ~2.6 kb) and nuclear *Rag*2 sequences (~1.4 kb) were obtained from previously published studies (Lewis Oritt *et al*., 2001; Van Den Bussche & Hoofer, 2001; Van Den Bussche *et al*., 2002b). Cytochrome *b* sequences generated for the present study are given below. The first number in parentheses corresponds to the tissue sample at the Ambrose Monell Cryogenic Collection (AMCC) and the second number identifies the cadaver voucher specimen at the Mammalogy Department-Division of Vertebrate Zoology, both at the American Museum of Natural History (AMNH). The collecting locality follows the specimen numbers for each individual. *Mormoops blainvillei* (102762, 274611): Jamaica, Westmoreland, Revival, Monarva Cave; *P. parnellii* (110395, 269115): French Guiana, Cayenne, Paracou, near Sinnamary; (103048, 269115): Dominican Republic, María Trinidad Sánchez, La Entrada (de Cabrera); (103050, 275497): Dominican Republic, María Trinidad Sánchez, La Entrada (de Cabrera); (102714, 274627): Jamaica, St Catherine, Polly Ground, St Clair Cave; *P. quadridens* (103036, 275500): Dominican Republic, María Trinidad Sánchez, La Entrada (de Cabrera); (102720, 274633): Jamaica, St Catherine, Polly Ground, St Clair Cave; (102335, wing puncture): Puerto Rico, Arecibo, Mata de Plátano; *P. macleayii* (102719, 274632): Jamaica, St Catherine, Polly Ground, St Clair Cave.

For outgroup comparison, sequences from *M. tuberculata* (GenBank accession nos. AF263222, AY141021, AF144068), *Noctilio leporinus* (AF263224, AF316477, AF330796), *Noctilio albiventris* (AF263223, AF330810, AF330803), and *Artibeus jamaicensis* (NC002009, AY011963) were used. Sequences from *Saccopteryx bilineata* (AF263213, AY141015, AF044664) were included in phylogenetic analyses to root the tree.

MOLECULAR DATA

For all specimens, DNA was isolated from wing clip or liver tissue that had been frozen or preserved in ethanol or lysis buffer in the field. DNA was extracted using a Qiagen DNeasy Tissue Extraction Kit (Qiagen, Inc.) following the manufacturer's protocol. Extracted DNA was used as a template in polymerase chain reaction (PCR) reactions with protocols and primers for the complete cytochrome *b* as described previously (Dávalos & Jansa, 2004). Amplification products were sequenced with the same primers used for PCR ampli-

fication. Sequencing reactions were purified through a $MgCl_2$–ethanol precipitation protocol and run on an ABI 3100 automated sequencer. Sequences were edited and compiled using Sequencher 4.1 software (GeneCodes, Corp.). Base-calling ambiguities between strands were resolved either by choosing the call on the cleanest strand or using the appropriate IUB ambiguity code if both strands showed the same ambiguity. Molecular sequences generated as part of this study have been deposited in GenBank under accession numbers AY604454-AY604462 (Appendix).

Morphological data

The morphological character matrix of Simmons & Conway (2001) was appended to the molecular data to generate combined analyses of all characters available for the group, and investigate character conflict among different sources of data. The concatenation of molecular and morphological data was justified because Simmons & Conway (2001) examined specimens of all recognized subspecies (Table 1).

Data analysis

Protein-coding cytochrome *b* and *Rag*2 sequences were aligned by eye using Sequencher 4.1 (GeneCodes, Corp.). Unlike those two genes, mtrDNA does not code for protein products and sequence length varies among taxa, and even individuals. Positional homology of the sequence alignment is an assumption of phylogenetic analysis (Swofford *et al.*, 1996). CLUSTAL W (Thompson, Higgins & Gibson, 1994) was used to infer sequence homology in these sequences, with a gap/substitution penalty of 10 : 1. The resulting alignment was adjusted manually based on secondary structure models that take into account the functional role of these mitochondrial regions in protein synthesis (Springer & Douzery, 1996; Burk, Douzery & Springer, 2002). Where sequence homology could not be unambiguously established by this method, the characters were excluded from subsequent phylogenetic analyses. The resulting alignment is available from the author upon request.

To describe the variation in cytochrome *b* among taxa uncorrected pair-wise distances were calculated using PAUP* 4.0b10 (Swofford, 2002). Cytochrome *b* sequences were also examined for fixed character differences among putative taxonomic units, subspecies *sensu* Smith (1972). Sequences of each subspecies were compared against sequences of other subspecies in the same species, and the number of fixed character differences that distinguished them was scored.

Parsimony analyses of the morphological, cytochrome *b*, mtrDNA, and *Rag*2 datasets were performed separately and on combined matrices using branch and bound searches as implemented in PAUP*. For each search, phylogenetically informative characters were treated as unordered and equally weighted, and gaps were treated as missing data. Clade stability was assessed using the nonparametric jackknife and the Bremer support index (Bremer, 1994). All parsimony jackknife analyses included 1000 replicates; searches were heuristic with ten replicates of random taxon addition followed by tree bisection reconnection branch swapping. Bremer values were calculated with the aid of AutoDecay v. 4.0.2 (Eriksson, 1999). The Templeton (1983) test implemented in PAUP* was used to assess whether topologies differ significantly on how well they fit each data partition.

Best-fit maximum likelihood models for molecular data were selected using nested likelihood ratio tests as implemented in MODELTEST v. 3.06 (Posada & Crandall, 1998). Maximum likelihood analyses of the different molecular data sets were performed using PAUP*. Finally, the constancy in rates of molecular evolution throughout the tree was evaluated. To provide the most conservative test for a clock-like model of evolution, a UPGMA tree based on Jukes–Cantor distances was calculated, and the likelihood scores of the best-fit model without enforcing the clock ($\log L_1$), and the same model forcing a clock ($\log L_2$) were compared. The significance of the difference in likelihood scores was tested by comparing $-2\log\Lambda$ against a χ^2 distribution (d.f. = $N_{\text{taxa}} - 2$). If the value for $-2\log\Lambda$ was significant, then the molecular clock could be rejected. Subsequent to model selection, the maximum likelihood tree was determined using a heuristic search in which the parameter values under the best-fit model were fixed and a Neighbour-joining tree was used as a starting point for TBR branch swapping. Likelihood nonparametric jackknife analyses included 300 nonrate-constant replicates, with a neighbour-joining starting tree followed by subtree pruning regrafting branch swapping in heuristic searches.

Bayesian methods were used to estimate a phylogeny applying different models of molecular evolution for each partition of the molecular data. This analysis featured three partitions, noncoding mitochondrial DNA, protein-coding mtDNA, and nuclear DNA. The model of sequence evolution was determined using MODELTEST (see above). The values for model parameters were treated as unknown variables to be estimated in each analysis and allowed to vary between partitions. Bayesian analysis was conducted using MrBayes v. 3.0b4 (Huelsenbeck & Ronquist, 2001), with random starting trees without constraints, four simultaneous Markov chains run for 2 000 000 generations, trees sampled every 100 generations, and temperature set to 0.20. Resulting burn-in values were determined empirically by evaluating tree likelihood scores and estimated parameters. Analyses were repeated in four separate

runs to ensure that trees converged on the same topology and similar parameters.

Biogeographical analyses

The biogeographical hypotheses of Smith (1972) and Czaplewski & Morgan (2003) were compared with the results of phylogenetic analyses from different data sources using several methods. The significance in length differences between obtained phylogenies and biogeographical predictions in parsimony was measured using the Templeton (1983) test. Two likelihood-based topology tests were applied: the nonparametric Shimodaira & Hasegawa (1999) test, and a parametric bootstrap (Goldman, Anderson & Rodrigo, 2000). The Shimodaira & Hasegawa (1999) one-tailed test resamples the data by bootstrapping to construct a distribution of log likelihoods and then compares the specified trees with this distribution. The question is whether the differences between obtained trees and trees derived from biogeographical hypotheses fall beyond the distribution from resampled trees.

For the parametric bootstrap, the model parameters obtained using MODELTEST for each molecular partition and for the concatenated molecular data and their corresponding optimal topology were employed to simulate 100 data sets using SEQ-GEN v. 1.2.7 (Rambaut & Grassly, 1997). PAUP* was then used to optimize trees for each of the simulated data sets with and without topological constraints corresponding to biogeographical models. The difference between maximum likelihood scores for constrained and unconstrained trees using the actual data was then compared with the distribution of differences based on simulations.

The predictions regarding the relative ages of divergence between clades were tested by generating confidence intervals around branch lengths using the results of the parametric bootstrap. The branch lengths for each of the simulated datasets under optimal rate-constant maximum likelihood parameters within each data partition were tabulated, and used to calculate the 95% confidence limit around the nodes of interest.

Dispersal-vicariance analysis, DIVA (Ronquist, 1997), was used to estimate ancestral areas. DIVA reconstructs the ancestral distribution at each of the internal nodes of a given phylogeny. This is accomplished by means of optimization rules and set costs for extinction (cost of 1 per area lost) and dispersal (cost of 1 per area added). Vicariant and sympatric speciation carry no cost. The ancestral area estimate can be constrained to contain any minimum number of areas. Species distributions are therefore explained by assigning costs for each event in a way that biogeographical explanations imply the least possible cost.

RESULTS

Sequence variation and saturation analysis

MtrDNA

Alignment of 12S rRNA, $tRNA^{val}$, and 16S rRNA genes resulted in 2677 aligned positions of which 30 were excluded from phylogenetic analyses because they potentially violated hypotheses of positional homology. Within the remaining 2647 sites, 971 (37%) of sites were variable and 677 (26%) were parsimony informative. The average base composition of sequences was skewed, with a deficiency of guanine (17.8%) and an overabundance of adenine (36.0%). This bias in base composition did not differ significantly across taxa (χ^2 test implemented in PAUP*, $P = 0.666$).

Cytochrome b

Complete cytochrome *b* sequences were obtained for all taxa, with the exceptions of *Mystacina* (AF144068) and *Saccopteryx* (AF044664), for which only 402 base pairs were available from GenBank. Because one of the objectives of this study was to assess the intraspecific variation of Caribbean species, several individuals per mormoopid species were included in the cytochrome *b* analysis (Table 1). Of these, two *P. parnellii* individuals from different localities in Jamaica (AMCC102714 = AY604456, TK27704 = AF338661), and two *P. quadridens* from the same Jamaican cave (AMCC102720 = AY604458, TK9487 = AF338682) had identical sequences (Appendix). A summary of the uncorrected pair-wise divergences among individuals in different taxonomic ranks is shown in Figure 2. Table 2 summarizes the results of sequence examination for fixed character differences among currently recognized subspecies within species *sensu* Smith (1972).

Within cytochrome *b* of the ingroup, 460 (40%) of sites were variable and 421 (37%) were parsimony informative. The distribution of the parsimony-informative sites was highly dependent on codon position: 19.2% in first, 4.8% in second, and 76.0% in third codon position. Most substitutions were synonymous, and translation of sequences to amino acids led to a matrix with only 68 informative sites (21.0% variable sites, among which 85.0% were parsimony informative). The average base composition of sequences was skewed. There was little bias at first codon position, and a deficiency of adenine (20.3%) and guanine (13.7%) and an overabundance of thymine (40.6%) for second position. The third position showed a strong bias: a deficiency of guanine (4.0%) and thymine (14.0%), and an abundance of adenine (42.1%) and cytosine (39.8%). The bias in base composition did not differ significantly across taxa when the whole cytochrome *b* gene was considered (χ^2 test implemented in PAUP*, $P = 0.996$). Similar results were obtained for

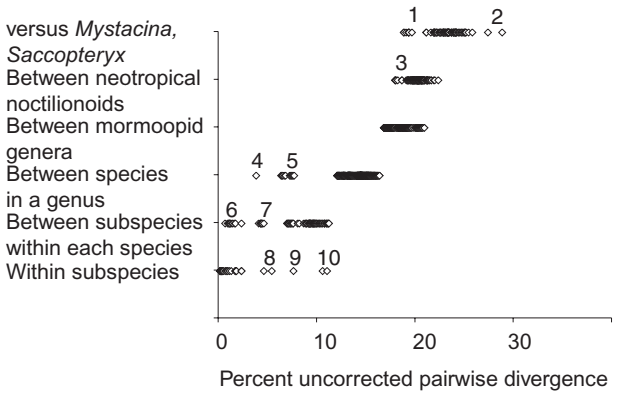

Figure 2. Scatter plot of uncorrected sequence divergence in cytochrome *b* against taxonomic rank. Taxonomy follows Smith (1972). Numerals indicate cytochrome *b* distance outliers: 1: with respect to *Saccopteryx*; 2: between *Mystacina* and *Noctilio*; 3: between *Mormoops* and *Artibeus*; 4: between *Noctilio albiventris* and *Noctilio leporinus*; 5: between *Pteronotus davyi* and *Pteronotus gymnonotus*; 6: between currently recognized subspecies of *Pteronotus quadridens*, *Pteronotus macleayii*, and *Mormoops megalophylla*; and also between *Pteronotus parnellii* from Mexico, Guatemala and Honduras classified in the subspecies *mesoamericanus* and *mexicanus*; 7: between *P. parnellii* from Puerto Rico and Hispaniola, and among samples from Guyana, Mexico and Honduras; 8: between *Pteronotus personatus* from Suriname, and individuals from Venezuela and Guyana; 9: between *P. parnellii* individuals from French Guiana and Suriname; and 10: between *P. parnellii* individuals from Guyana, and Suriname and French Guiana.

first and second positions separately, but not for third codon position, where the test was significant at the 0.1% level ($P = 0.000$) among all taxa, and at the 5% level ($P = 0.048$) within the ingroup.

Heterogeneity in base composition across taxa is known to affect phylogenetic reconstruction (Lockhart *et al.*, 1994): bias in third codon position, which contains most of the sequence variation, may confound the results of sequence analyses. To examine this hypothesis, the most divergent taxon in GC content of third codon positions of cytochrome *b* was identified (GC content average for all taxa = 43.8%, SD = 4.8): *Artibeus jamaicensis* (31.6%). It can be assumed that the heterogeneity in base composition of this outgroup taxon is not affecting the analysis because no other taxon exhibits similar variation. For the ingroup, no difference in base composition was found within *Mormoops* (χ^2 test implemented in PAUP*, $P = 1.00$), or *Pteronotus* (χ^2 test implemented in PAUP*, $P = 1.00$). Heterogeneity in third codon base composition was confined to comparisons between the two genera. Data sources other than third codon positions in cytochrome *b* (e.g. morphology, mtrDNA, *Rag*2) all support the reciprocal monophyly of each mormoopid genus. Base composition heterogeneity in third codon positions was not presumed to distort phylogenetic analyses toward recovering monophyletic genera.

Graphs of transitions and transversions for each codon position vs. uncorrected total sequence divergence were plotted to assess saturation in sequences. Those curves (not shown) indicated that first and second codon position did not experience multiple transition or transversion substitutions. Third codon positions showed saturation in transition and transversion substitutions for *Saccopteryx* and *Mystacina*, in part because their sequences were incomplete.

Rag2

Of the sequences available, two *Mormoops megalophylla* individuals (CN98443 = AF338702, TK27640 = AF330818), two *Pteronotus davyi* individuals (CN101305 = AF338691, TK25127 = AF338692), and two *P. quadridens* individuals (TK32171 = AF338695, TK9487 = AF338696) had identical sequences (see Appendix for localities). Of the 1398 *Rag*2 sites, 252 (18%) were variable and 157 (11%) were parsimony informative. The distribution of the parsimony-informative sites was highly dependent on codon position: 16.6% in first, 8.9% in second, and 73.9% in third codon position. Most substitutions were synonymous, and translation of sequences to amino acids led to a matrix with only 41 informative sites (15.2% variable sites, among which 57.7% are parsimony informative). The average base composition of sequences was skewed, with a deficiency of cytosine (18.1%) and thymine (20.4%) and an overabundance of adenine (30.6%) in first codon position. Second positions showed a deficiency of guanine (17.9%) and an overabundance of adenine (35.0%), while third positions showed a deficiency of guanine (16.8%) and an overabundance of thymine (31.0%). The biases in base composition did not differ significantly across taxa for the whole gene, or for different codon positions ($P = 1.000$).

PHYLOGENETIC ANALYSES

Four data sets were included in phylogenetic analyses: (1) the mitochondrial cytochrome *b*; (2) mtrDNA (12S, $tRNA^{val}$, and 16S); (3) a fragment of the nuclear *Rag*2; and (4) the morphological character matrix for mormoopids published by Simmons & Conway (2001); see also Table 1 and the Appendix. Sequences from different genes were concatenated for combined analyses from the same individuals when possible (Appendix). Maximum parsimony analyses of individual data sets (Figs 3, 4) and the combined 'total evidence' data matrix (Fig. 4) were conducted with all unordered and unweighted characters.

Table 2. Fixed character differences (FCD) in cytochrome *b* base pairs among subspecies and selected populations within each currently recognized species

Taxon 1	*N*1	Taxon 2	*N*2	FCD
Mormoops megalophylla megalophylla	4	*Mormoops megalophylla tumidiceps*	1	11
Mormoops blainvillei Cuba	1	*Mormoops blainvillei* Jamaica	2	4
Pteronotus parnellii parnellii Jamaica	2	*P. parnellii* other localities	23	19
Pteronotus parnellii pusillus	2	*Pteronotus parnellii* other localities	23	8
Pteronotus parnellii portoricensis	2	*Pteronotus parnellii* other localities	23	6
Pteronotus parnellii parnellii, *P.p. portoricensis*	4	*Pteronotus parnellii* other localities	21	4
Pteronotus parnellii mexicanus	2	*Pteronotus parnellii* other localities	23	3
Pteronotus parnellii mesoamericanus	2	*Pteronotus parnellii* other localities	23	1
P. parnellii rubiginosus Guyana	1	*Pteronotus parnellii* other localities	24	4
Pteronotus parnellii mexicanus, *P.p. mesoamericanus*, *P.p. rubiginosus* Guyana	6	*Pteronotus parnellii* other localities	19	8
Pteronotus parnellii rubiginosus Suriname	1	*Pteronotus parnellii* other localities	22	15
Pteronotus parnellii rubiginosus French Guiana	1	*Pteronotus parnellii* other localities	22	21
Pteronotus parnellii rubiginosus Suriname & French Guiana	2	*Pteronotus parnellii* other localities	21	7
Pteronotus macleayii macleayii	1	*Pteronotus macleayii griseus*	2	11
Pteronotus quadridens quadridens	1	*Pteronotus quadridens fuliginosus*	4	1
Pteronotus quadridens Cuba and Jamaica	3	*Pteronotus quadridens* Puerto Rico and Hispaniola	2	8
Pteronotus personatus personatus	3	*Pteronotus personatus psilotis*	2	9
Pteronotus personatus Guyana & Venezuela	2	*Pteronotus personatus* other localities	3	13
Pteronotus personatus Guatemala	1	*Pteronotus personatus* other localities	4	15
Pteronotus personatus Mexico	1	*Pteronotus personatus* other localities	4	41
Pteronotus davyi davyi	4	*Pteronotus davyi fulvus*	3	55
Pteronotus davyi	7	*Pteronotus gymnonotus*	3	20

N, Sample size. Taxonomy follows Smith (1972). For complete geographical distribution of subspecies, see Table 1.

The Templeton (1983) tests indicated there were significant differences in the fits of cytochrome *b* to the *Rag*2 ($P = 0.047$) and morphology trees ($P = 0.020$); the fits of the mtrDNA to the cytochrome *b* ($P = 0.019$) and *Rag*2 ($P = 0.036$) trees; the fits of *Rag*2 to the cytochrome *b* ($P = 0.076$) and morphology trees ($P = 0.014$); and the fits of the morphology to the cytochrome *b* ($P = 0.009$) and *Rag*2 ($P = 0.023$) trees. This test is not being used as a criterion for combining or excluding data, but to investigate conflict between data sets. The alternative topologies of Figures 3, 4, and the support for competing hypotheses (Table 3) further confirm these statistical results. Conflict among data sets does not appear to undermine phylogenetic resolution when combining data (Fig. 4).

The models of molecular evolution and parameters selected for each data set using MODELTEST are shown in Table 4. The estimates of phylogeny given the parameters of Table 4 for each molecular data partition, the concatenated molecular data set, and the combined molecular and morphological data are shown in Figures 3, 4. Bayesian methods were used to obtain an estimate of phylogeny that accounted for three models of sequence evolution (Table 4) while using all available molecular data. Exemplars having the broadest character sampling from each named population in Figure 3 were used as terminals in this analysis. Individual partitions coded as 'all missing' if no sequences were available for a given exemplar. Stationarity in parameter estimation was reached after 100 000 generations (burn in = 1000 trees). The resulting trees are summarized in Figure 5.

Comparison with previous studies

Recent studies of mormoopid phylogeny provided most of the data analysed here (Lewis Oritt *et al*., 2001; Simmons & Conway, 2001; Van Den Bussche *et al*., 2002b). The monophyly of the family and its genera could be questioned based on some of the data partitions analysed separately (Kennedy *et al*., 1999) (Table 3, Fig. 3). This result can be explained by homoplasy of those data for deep divergences, rather than as a phylogenetic signal about mormoopid relationships. For the purpose of the present study, the monophyly of mormoopids, and of *Mormoops* and *Pteronotus*, will be assumed because

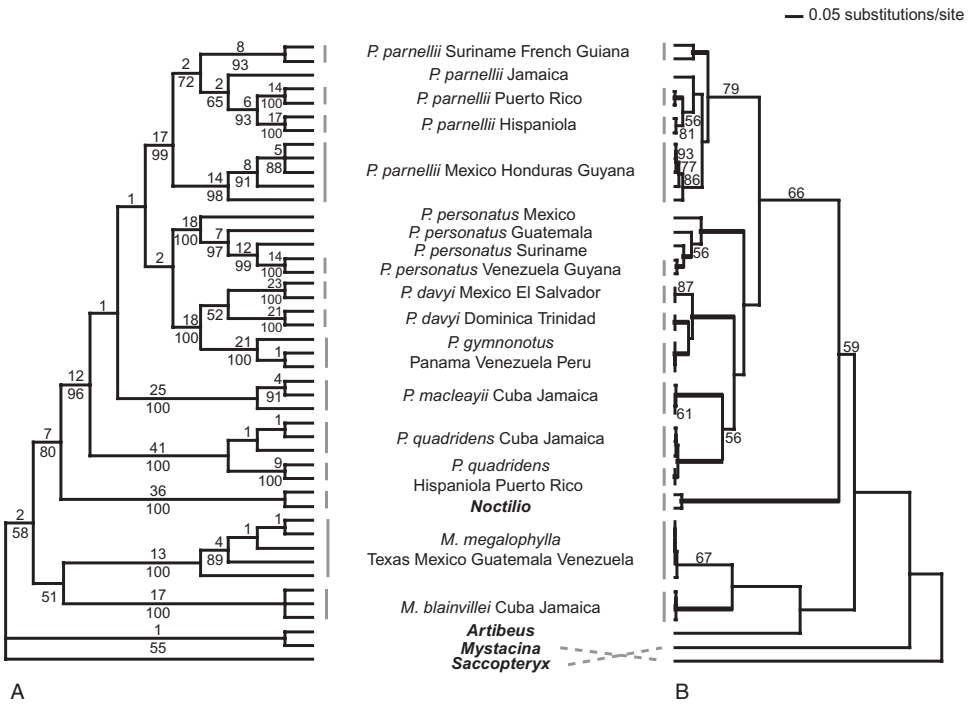

Figure 3. A, strict consensus of eight most parsimonious cladograms resulting from analysis of cytochrome *b* ($L = 1792$ steps, consistency index = 0.439, retention index = 0.775). Numbers below branches are Bremer support values, above branches are percent of 1000 jackknife replicates. Names of outgroups are in bold; for sequence data, see Appendix. B, phylogram resulting from maximum likelihood analysis using a rate-constant GTR+I+Γ model of DNA evolution ($-\ln L = 9181.23$). Numbers above or below branches are percent of 300 50% jackknife replicates, thicker lines indicate 100% jackknife support.

Table 3. Support for relationships among mormoopids

Node/dataset	cyt *b*	mtrDNAA	*Rag*2	Morphology	Total	Supported by:
(*Mormoops*, *Pteronotus*)	5	5/83	59/1	9/98	19/98	All but cyt *b*
Mormoops	0/51	46/100	98/8	20/100	102/100	All
Pteronotus	12/96	20/100	97/6	10/99	67/100	All
(*davyi*, *gymnonotus*)	18/100	43/100	99/8	4/90	73/100	All
(*quadridens*, *macleayii*)	46	11/92	96/6	1/48	26/100	All but cyt *b*
parnellii sister to all other *Pteronotus*	29	4/55	91/5	33	10/82	*Rag*2 mtrDNA
(*parnellii*, *personatus*)	23	29	2	19	17	None
(*parnellii* (*davyi*, *gymnonotus*))	4	1	0	19	0	None
(*parnellii* (*quadridens*, *macleayii*))	7	3	1	1	5	None
((*davyi*, *gymnonotus*) (*quadridens*, *macleayii*))	0	23	65/2	20	19	*Rag*2
(*personatus* (*davyi*, *gymnonotus*))	2/36	18	24	0	20	None
(*personatus* (*quadridens*, *macleayii*))	1	36	3	1/53	3/44	Morphology

Relationships are represented using the Newick format. Values are Bremer support/jackknife; when only one number is shown, it corresponds to jackknife.

this is the best-supported conclusion given all the evidence at hand (Table 3, Figs 4, 5). For two nuclear exons that do not support mormoopid monophyly, see Van Den Bussche, Hoofer & Hanson (2002a) and Van Den Bussche *et al.* (2003).

Within *Pteronotus*, there is strong support for sister taxa relationships between *P. quadridens* and *P. macleayii*, and between *P. davyi* and *P. gymnonotus* (Figs 3–5); see also Lewis Oritt *et al*. (2001), Van Den Bussche *et al*. (2002b), and Van Den Bussche &

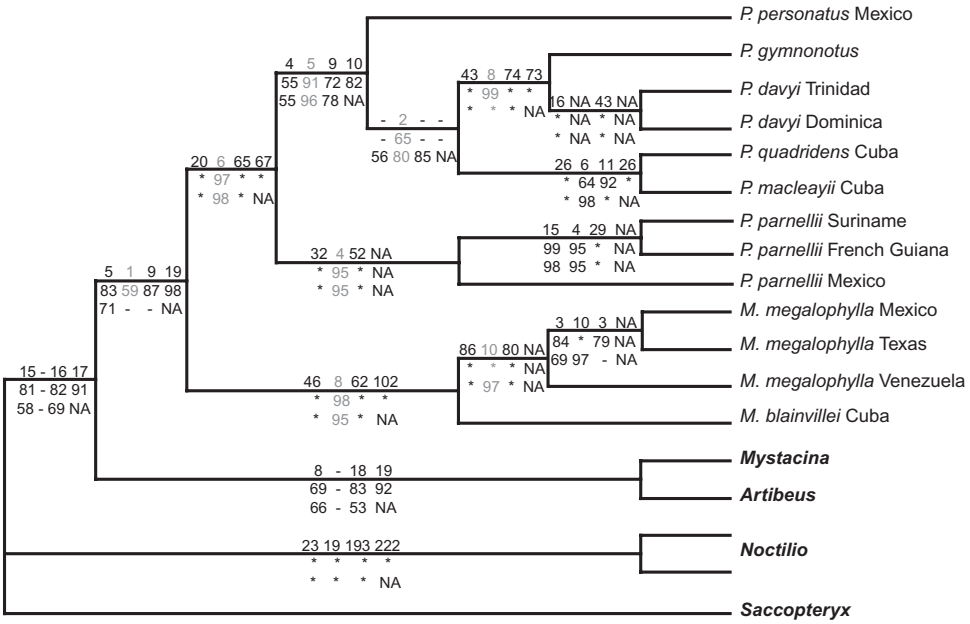

Figure 4. Cladogram resulting from maximum likelihood analysis of concatenated mitochondrial ribosomal DNA, cytochrome *b*, and *Rag*2 sequences ($-\ln L = 24736.88$). Sequences for at least two of the molecular partitions were available for each terminals. Support values are shown for mtrDNA in the first column, *Rag*2 in the second column, concatenated molecular sequences in the third column, and total evidence in the fourth column. The top row shows Bremer support indices; second row is the percent of 1000 50% jackknife pseudoreplicates using parsimony; and the third row is the percent of 300 50% jackknife pseudoreplicates using maximum likelihood. Asterisks indicate jackknife support values of 100%. Dashes indicate that the data set does not resolve the branch, or does not support the resolution shown (Table 3). NA, not applicable; indicating the partition contains data for only one terminal and the branch could not be scored, or no maximum likelihood analysis including morphological data was performed. Numbers in grey indicate that the data partition does not include all terminals in the branch. Models of sequence evolution used to analyse each partition and resulting log-likelihood values are shown in Table 4. Names of outgroups are in bold; for sequence data, see Appendix.

Weyandt (2003). The position of *P. parnellii* as sister to all other *Pteronotus*, although not as well supported as previously discussed nodes (Table 3, Fig. 4), is better supported than any alternative placement of *parnellii* (Table 3). Finally, relationships among *Pteronotus personatus* and the clades formed by *davyi* and *gymnonotus*, and *quadridens* and *macleayii* are barely resolved (Fig. 4, but see Fig. 5).

There are three alternative hypotheses of relationships for the lineages of *personatus*, *davyi*, and *quadridens*. First, the sister relationship between *personatus*, and *davyi* and *gymnonotus*, is not strongly supported by any individual data set (Table 3, Figs 3, 4), and can be dismissed. Of the remaining two alternatives, a sister relationship between *personatus*, and *quadridens* and *macleayii* is supported by morphology (Simmons & Conway, 2001), and this is the resolution of the total evidence tree (not shown). A sister relationship between *davyi* and *gymnonotus*, and *quadridens* and *macleayii* is supported by *Rag*2, maximum likelihood analysis of mtrDNA, and Bayesian phylogeny estimation (Table 3, Fig. 3B–5); see also Van Den Bussche & Weyandt (2003). Both topologies were considered in inferring ancestral areas.

Biogeographical Analyses

Table 5 summarizes the differences between obtained topologies and a tree constrained to make the Caribbean *P. parnellii* be sister to the Central American *P. parnellii* (only applicable to the cytochrome *b* data), *quadridens* and *macleayii* be sister taxa, and this latter clade be sister to *P. personatus* (Smith, 1976). The confidence intervals around relevant divergences, estimated using the molecular evolution models of Table 4, are presented in Figure 6. Ancestral area estimates are shown in Figure 5.

DISCUSSION

Basal units in the Mormoopidae

The species diversity of the mormoopids has been underestimated. Two hypotheses underlie competing

Table 4. Models of molecular evolution and parameters selected for each molecular data set (see Table 2 for sequences)

Data	Model	*R*-matrix	α	I	–2logΛ	d.f.	*P*
ML mtrDNA	GTR+I+Γ	1.0, 3.3, 1.0, 1.0, 10.7	0.4090	0.3347	24.2	16	> 0.05
Bayes mtrDNA	GTR+I+Γ	7.9 (3.6–13.8), 12.2 (5.6–20.9), 5.5 (2.5–9.6), 0.3 (0.0–1.0), 48.3 (23.1–83.0)	0.421 (0.260–0.599)	0.296 (0.156–0.426)	–	–	–
ML cyt *b*	GTR+I+Γ	0.5, 9.7, 0.5, 0.3, 10.4	0.9773	0.5040	52.4	43	> 0.05
Bayes cyt *b*	GTR+I+Γ	0.7 (0.1–1.7), 13.8 (3.9–32.4), 0.9 (0.0–2.4), 0.7 (0.0–2.0), 21.1 (5.3–51.7)	0.851 (0.647–1.068)	0.507 (0.470–0.544)	–	–	–
ML *Rag*2	GTR+Γ	1.0, 5.1, 1.0, 1.0, 7.8	0.2433	–	26.2	18	> 0.05
Bayes *Rag*2	GTR+Γ	3.1 (1.1–5.7), 8.8 (3.7–15.5), 1.0 (0.2–1.9), 2.1 (0.6–4.2), 13.3 (5.5–26.6)	0.265 (0.146–0.393)	–	–	–	–
ML molecular	GTR+I+Γ	6.5, 11.7, 4.1, 1.0, 37.0	0.4505	0.3820	43.1	16	< 0.001

Bayes, parameters used in Bayesian analysis of concatenated data; GTR, general time reversible model; ML, parameters used in maximum likelihood analyses; *R*-matrix, rate matrix parameter (with respect to G-T transversion); α, shape parameter, I, proportion of invariant sites; –2logΛ, 2[log$L1$ – log$L2$], where $L1$ = likelihood without clock and L_2 = likelihood with clock. Parameters obtained from Bayesian analyses are followed by the 95% confidence interval (in parentheses).

assessments of species diversity. The first hypothesis assumes populations of widespread species as part of a continuum of differentiation that appears great at the extremes, but is only slight between adjacent groups (Koopman, 1955). Although some populations are allopatric, it is assumed that gene flow among them exists or occurred until recently. Because morphological intergradation (used to infer gene flow) among insular and continental populations is not observed, the range of (non)resemblance permitted in a given species has been widened (Smith, 1972).

The assessment of sequence variation among putative units (subspecies) within the mormoopids (Table 2) revealed multiple instances of characters that appear to be fixed in cytochrome *b*. These molecular data support a second hypothesis: gene flow between insular and continental populations appears to have ceased even before fully recognized biological species (e.g. *P. gymnonotus* and *davyi*; Fig. 3B) evolved into separate lineages. The subtle morphological differences dismissed under a presumption of gene flow provide evidence for the isolation and independent evolution of separate lineages in widespread species such as *parnellii*, *davyi*, and *personatus*. Because sampling sizes for molecular markers were small, these differences alone cannot provide species limits. In some instances, molecular character differences, high sequence divergence among presumed conspecifics (bottom two tiers of Fig. 2), distributional ranges that encompass broad areas separated by water and land barriers (Table 1, Fig. 1), and taxonomic limits based on morphological variation (Smith, 1972) coincide and strengthen the hypothesis of evolutionary independence. These criteria (Tables 1 and 2) apply to named island populations of *P. parnellii*: *parnellii* (Gray, 1843), *pusillus* (Allen, 1917), and *portoricensis* (Miller, 1902); the continental *P. parnellii* ranging from Mexico to Guyana currently classified in the subspecies *mexicanus* (Miller, 1902), *mesoamericanus* (Smith, 1972), and *rubiginosus* (Wagner, 1843); the currently recognized subspecies of *P. davyi*: *davyi* (Gray, 1838) and *fulvus* (Thomas, 1892); and subspecies of *P. personatus*: *personatus* (Wagner, 1843) and *psilotis* (Dobson, 1878). Each of these populations should be considered as a species, named using the subspecies taxonomy. The name *Pteronotus rubiginosus* (Wagner, 1843) precedes *mexicanus* and *mesoamericanus*, and applies to the continental bats in the *P. parnellii* lineage as described above (note that the status of *fuscus* and *paraguanensis* was not evaluated; Table 1). Both cytochrome *b* (Table 2) and *Rag*2 (Lewis Oritt *et al.*, 2001) showed differentiation in Mexican and Central

Table 5. Significance of topological differences and number of extra steps necessary to fit the biogeographical hypothesis of Smith (1972)

Data	Test	Length difference	Significance
cyt *b*	MP*	18	$P = 0.01$
	SH		$P = 0.55$
	PB		$P = 0.80$
mtrDNA2	MP	0	–
	SH		$P = 0.13$
	PB		$P = 0.53$
*Rag*2†	MP	5	$P = 0.06$
	SH		$P = 0.13$
	PB		$P = 0.40$
Molecular†	MP	0	–
	SH		$P = 0.78$
	PB		$P = 0.99$
Total†	MP	0	–

*Length difference arises from constraining (*parnellii* Caribbean, *parnellii* Mexico, and Central America), and not from relationships between *quadridens* and *macleayii*, and their sister taxon. †Differences pertain the constraint [(*quadridens*, *macleayii*), *personatus*] only. MP, maximum parsimony (number of extra steps and significance in Templeton (1983) test; PB, parametric bootstrap (maximum likelihood); SH, Shimodaira & Hasegawa (1999) test (maximum likelihood).

American populations of *P. psilotis*. Further sampling is necessary to determine if characters are fixed because taxonomic conclusions derived from single molecular exemplars would be suspect.

Mitochondrial cytochrome *b* from samples of *Pteronotus rubiginosus* and *P. personatus* from northern South America west of Guyana is distinct from that sampled east of Guyana (Suriname and/or French Guiana; Table 2, Fig. 1). These character differences and attendant levels of sequence divergence had not been anticipated in the morphological study of Smith (1972). French Guianan specimens of *P. parnellii* can also be distinguished from those from the remainder of the range by their larger size (Simmons & Voss, 1998). In Venezuela, *P. paraguanensis* appears to have become isolated as a result of breaks in the humid forest (Gutiérrez, 2004). This mechanism might explain the differentiation observed, but greater geographical and character sampling is needed to investigate these (possibly) cryptic species, and test the possibility that accelerated rates of sequence evolution have led to this pattern (although this is unlikely, see Table 4).

In *P. quadridens* discontinuous variation in cytochrome *b* occurs between Cuba and Jamaica, and Hispaniola and Puerto Rico, rather than coinciding with the subspecies taxonomy that separates Cuban from other Greater Antillean bats (Tables 1, 2). These taxa are not elevated to species here, despite the possible geographical isolation by ocean barriers, because sampling was sparse, the molecular differentiation does not match subspecies boundaries based on morphology, and no differences were detected in *Rag*2. For the purpose of estimating ancestral areas, each terminal that appears with a name in Figure 3 was treated as a separate taxon.

Biogeography of the Mormoopidae

The P. parnellii lineage (subgenus Phyllodia)

The molecular phylogeny challenges the biogeographical hypothesis of Smith (1972) on the single, Middle American origin of Antillean populations. Lewis Oritt *et al*. (2001) first proposed northern South America as the ancestral area of Antillean *Phyllodia*, but this result is not significantly different from the traditional biogeographical explanation [except when using the Templeton (1983) test; Table 5]. The phylogeny of Figure 5 is the first to suggest that *P. parnellii* is not sister to a clade containing *P. pusillus*. Because both trees (Figs 3B, 5) are equally good at explaining the data ($P = 0.352$, Shimodaira–Hasegawa test), *Phyllodia* might have reached the Caribbean or the continent more than once. Two *Phyllodia* species have been recorded as Quaternary fossils on Hispaniola (Morgan, 2001; Table 1); the extant *pusillus* and sp. cf. *rubiginosus*; perhaps corresponding to separate waves of colonization from the continent and/or adjacent islands.

Whether bats in this lineage first arose on the islands or the continent cannot be established because both regions are optimized in the ancestral area (not shown). Furthermore, the low support values (Figs 3B, 5) mean that *parnellii*, *pusillus* and *portoricensis*, *rubiginosus*, or '*rubiginosus*' from Suriname and French Guiana could each be the oldest branch within the lineage, adding uncertainty to the geographical origin of the subgenus. The Caribbean-continent divergence within this lineage is as great as that between Surinamese and Guianan '*rubiginosus*' and sister clade (Fig. 6A). By contrast, sequence divergence within the widespread *rubiginosus* clade is significantly lower (Fig. 6A), as expected if the expansion to Middle America or north-western South America had happened recently.

Taken together, the results imply that the geographical history of these bats is more complex than proposed hitherto (Smith, 1972), and suggest avenues for future research. First, more rapidly evolving characters are needed to resolve relationships among the species in this subgenus (Figs 3, 5). Second, geographical sampling must include the entire range of *Phyllodia* because apparently continuous populations show

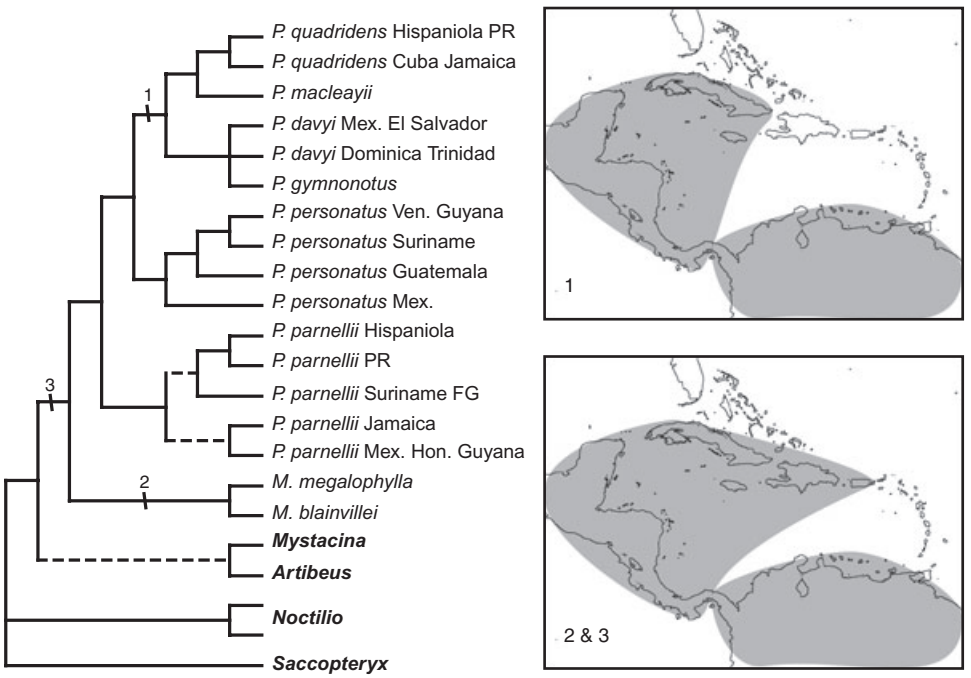

Figure 5. Majority rule (50%) consensus of 19 000 cladograms resulting from Bayesian analysis of concatenated molecular data for all diagnosable mormoopid taxa (– ln$L$ = 24 910; 95% confidence interval = 24,890–24 920). Dashed branches had posterior probabilities between 0.50 and 0.95. All other branches had posterior probabilities between 0.95 and 1. Names of outgroups are in **bold**; for sequence data, see Appendix. The top panel shows the ancestral area inferred for branch 1, the bottom panel shows the ancestral area of branches 2 and 3. DIVA Optimizations were constrained to a maximum of two areas, and all solutions are shown. Three alternatives to the polytomy of *Pteronotus davyi* and *Pteronotus gymnonotus*, two alternatives to the sister of *Pteronotus quadridens* and *macleayii* (*davyi* and *gymnonotus*, or *personatus*), and two taxonomies (the traditional species taxonomy of Smith (1972), or that shown in Figure 3 were analysed, and all result in the same composite estimates. Geographic distributions are as shown in Table 1. *Pteronotus pristinus* and *Mormoops magna* were not analysed. FG, French Guiana; Hon., Honduras; Mex., Mexico; PR, Puerto Rico; Ven., Venezuela.

deep divergences that might represent additional independently evolving lineages (e.g. in northern South America). Third, such studies should include morphological characters because the Caribbean *Pteronotus pristinus* (Silva-Taboada, 1974; Simmons & Conway, 2001) and *Pteronotus* sp. cf. *rubiginosus* (Morgan, 2001) are only known as fossils and might provide fresh insights into the history of exchange between the continental and insular Neotropics.

Other Antillean Pteronotus

Phylogenetic analyses including morphological data support the hypothesis of Smith (1972), whereby the *P. macleayii* and *quadridens* clade is sister to *P. personatus s.l.* (Table 3), while analyses of *Rag*2 result in the resolution of Figure 4. The difference between alternatives is not significant (Table 5), despite the posterior probability of 1.0 obtained for the latter resolution (Fig. 5). Regardless, the phylogenies optimize the distribution of the ancestral lineage to include the western Greater Antilles (Fig. 5). If distance between areas were an indication, Mexico and/or Central America would be the likely continental source (Fig. 1). Near-interconnections between the Antilles and Middle America during periods of low sea level might have facilitated dispersal (Smith, 1972; Griffiths & Klingener, 1988).

The biogeographical analysis, however, inferred northern South America as part of the ancestral area (Fig. 5). Each of the plausible sisters to *P. macleayii* and *quadridens* contains both Middle American [*fulvus* and perhaps *davyi* and *gymnonotus* (Table 1), or the two paraphyletic lineages in *psilotis* (Fig. 3)], and South American lineages (*davyi* and *gymnonotus*, or *personatus*). Divergences between these continental populations are often significantly smaller than between *P. macleayii* and *quadridens* and its continental sister (Fig. 6), suggesting dispersal to the Caribbean preceded range expansion within the continent by far (Czaplewski & Morgan, 2003). The direction of this expansion from north to south is in agreement with a Mexican and/or Central American origin for *personatus*

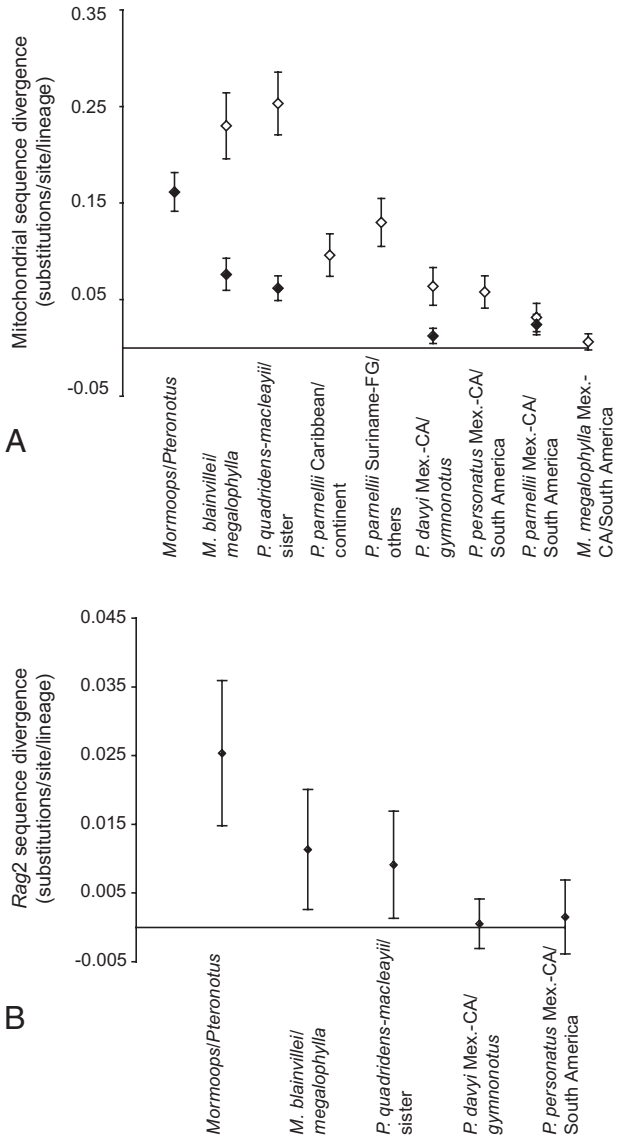

Figure 6. Confidence intervals around observed sequence divergence resulting from parametric bootstrapping of rate-constant mormoopid phylogenies. A, estimates of divergence for mitochondrial ribosomal DNA (black diamonds) and the cytochrome *b* gene (white diamonds). B, estimates of divergence for nuclear *Rag*2. CA, Central America; FG, French Guiana; Mex., Mexico.

s.l., and for the *macleayii* and *quadridens* clade if the two lineages were sister. The lack of resolution among *fulvus*, *davyi*, and *gymnonotus* precludes a firm conclusion but, if these three species all range into Middle America, then north-to-south range expansion would become parsimonious for this clade and its sister, despite the polytomy. This last question remains to be resolved because neither the northernmost range of *davyi* and *gymnonotus*, nor *P. davyi incae*, was sampled in molecular analyses (cf. Table 1, Appendix).

Mormoops and the Mormoopidae

The estimated ancestral area of *Mormoops* and the mormoopids (Fig. 5) encompasses both northern South America (Smith, 1972) and the Greater Antilles (Czaplewski & Morgan, 2003). The two biogeographical hypotheses are not mutually exclusive, and it is plausible that the most recent common ancestor of mormoopids was widespread from Mexico south to northern South America, and east to the Greater Antilles. Another interpretation of this result is that dispersal-vicariance analysis is inconclusive, and other sources of evidence are needed to clarify the geographical history of mormoopids.

There are several reasons to doubt that the ancestor of *Mormoops* was as widespread as estimated in Figure 5. First, extant *Mormoops* species do not overlap on the continent, but both are known from the Greater Antilles (albeit, one only as fossil). Second, one additional species, *Mormoops magna*, is known from late Pleistocene remains on Cuba (Silva-Taboada, 1974), adding a third *Mormoops* lineage to the Greater Antilles. Third, it is parsimonious to postulate that the ancestor of *Mormoops* reached the Greater Antilles before splitting into the extant species but, even if it did not, the divergence between the Antillean *blainvillei* and its sister taxon is significantly greater than that between *megalophylla* populations (Fig. 6A). The combination of species diversity and depth of divergence suggests *Mormoops* expanded its range from north to south.

If *Mormoops* ranged into the Greater Antilles even before *blainvillei* and *megalophylla* differentiated, Caribbean colonization in this family can be traced back to the divergence between the mormoopid genera, and might be as ancient as the Oligocene or Miocene (Czaplewski & Morgan, 2003). A northern neotropical (and perhaps insular) origin for the genus can be overturned by the discovery of a basal *Mormoops* species in South America. An extensive fossil record shows that *M. megalophylla* ranged from Florida through the Greater Antilles to Bahia in Brazil during the Late Pleistocene (Ray, Olsen & Gut, 1963; Silva-Taboada, 1974; Czaplewski & Cartelle, 1998). Studies of morphological variation are necessary to determine the relationships among extant and fossil *megalophylla* populations and test the hypothesis presented here because more than one species might be involved (Morgan, 2001).

One prediction following Czaplewski & Morgan's (2003) biogeographical model is borne by the molecular data: divergences between Antillean and continental mormoopids are greater than those between Central American and northern South American populations (Fig. 6). There is only one exception in the *P. parnellii* lineage (subgenus *Phyllodia*), where two northern South American populations might not share

a most recent common ancestor (Figs 3, 5). For every other mormoopid lineage, and even in one instance within *Phyllodia*, the divergence between Mexico/Central America and South America appears to be recent (Fig. 6), and might correspond to the completion of the Isthmus of Panama in the late Pliocene. Either Mexico/Central America or north-western South America was recently colonized by all mormoopid lineages. As discussed above, the direction of this expansion appears to be from north to south in *Mormoops* and *P. personatus s.l.*, but the evidence is ambiguous for *Phyllodia*, as well as for *P. davyi* and *gymnonotus*.

Because *Mormoops* is at the base of the mormoopid radiation, restricting its ancestral distribution to the northern Neotropics constrains the geographical origin of the family to that region. Other than differences in branch length (longer for northern neotropical splits, shorter for divergences between Mexico/Central America and South America), the fossil record also supports a north-to-south expansion. The oldest mormoopid diverged before the two extant genera (G. Morgan, pers. comm.), and ranged into Florida in the Oligocene (Czaplewski, Morgan & Naeher, 2003). In general, mormoopids appear to have reached South America late in their history, after diversifying in Mexico, Central America, and/or the Greater Antilles (Fig. 6).

This finding is critical to the biogeographical history of noctilionoids. Both morphology (Simmons & Conway, 2001) and large concatenated molecular datasets (Teeling *et al*., 2005) indicate that mormoopids and phyllostomids are each other's closest relative (this topology was not always recovered in this study, probably because taxon sampling among bat families was poor relative to the higher-level analyses cited above). Two phylogenetic hypotheses have been proposed to explain relationships among phyllostomids. One, based on analyses of mostly morphological data (Wetterer, Rockman & Simmons, 2000) identified the vampires (*Desmodus*, *Diaemus*, and *Diphylla*) as the oldest phyllostomid lineage. A second hypothesis based on mtrDNA and *Rag*2 (Baker, Porter, Hoofer & Van Den Bussche, 2003) suggests that *Macrotus* diverged before any other phyllostomid.

The geographical distribution of the basal lineage of the phyllostomids would have a disproportionate effect on ancestral area reconstructions for that family. Vampires range from Mexico to Chile and Uruguay, and fossils have been found on Cuba (Koopman, 1994). This lineage would not constrain the ancestral area of the phyllostomids because of its widespread distribution. Since the greatest diversity of phyllostomids is concentrated in northern South America and the vampires include it in their range, this would likely be the most parsimonious ancestral area for the family. By contrast, *Macrotus* is only known from the southwestern United States south to Guatemala, through the Greater Antilles and Bahamas (Koopman, 1994). If *Macrotus* is at the base of the phyllostomid radiation, then the ancestral distributions of mormoopids and phyllostomids were adjacent in the northernmost Neotropics. Phyllostomid fossils are known from the middle Miocene of La Venta (Czaplewski, 1997), indicating phyllostomids reached South America early in their history. The geographical distribution of these closely related families during their early history might help explain the remarkable differences in taxonomic and adaptive diversity between the two groups.

ACKNOWLEDGEMENTS

This article is based upon work supported by the National Science Foundation under Grant no. 0206336, it is a contribution from the Monell Molecular Laboratory and the Cullman Research Facility in the Department of Ornithology, American Museum of Natural History, and has received generous support from the Lewis B and Dorothy Cullman Program for Molecular Systematics Studies, a joint initiative of The New York Botanical Garden and the American Museum of Natural History. This research is supported by the Department of Mammalogy of the American Museum of Natural History, the NASA grant no. NAG5-8543 to the Center for Biodiversity and Conservation at the American Museum of Natural History, and the Department of Ecology, Evolution and Environmental Biology at Columbia University. Fieldwork was supported by the Ambrose Monell Cryogenic Collection and the Department of Mammalogy, both at the American Museum of Natural History, the Center for Environmental Research and Conservation and the Department of Ecology, Evolution and Environmental Biology, both at Columbia University, Elizabeth Dumont's NSF grant, and the Explorers' Club (New York). The author is currently supported by a NIH grant in bacterial genomics to H. Ochman at the University of Arizona. For comments, collecting permits, field or laboratory assistance, tissue loans, and/or as other intangible support, I thank F. K. Barker, A. S. P. Corthals, J. L. Cracraft, N. Czaplewski, M. Delarosa, R. DeSalle, A. Donaldson, K. Doyle, E. Dumont, R. Eriksson, J. Feinstein, N. Gyan, R. Harbord, S. A. Jansa, S. Koenig, J. Mercedes, J. C. Morales, G. S. Morgan, T. Nicole, A. L. Porzecanski, C. Raxworthy, A. Rodríguez, R. O. Sánchez, P. Schickler, M. Schwartz, N. B. Simmons, A. Tejedor, and A. Wright.

REFERENCES

Allen GM. 1917. Two undescribed West Indian bats. *Proceedings of the Biological Society of Washington* **30:** 165–170.

Baker RJ, Porter CA, Hoofer SR, Van Den Bussche RA.

2003. A new higher-level classification of New World leaf-nosed bats based on nuclear and mitochondrial DNA sequences. *Occasional Papers of the Museum of Texas Tech University* **230:** 1–32.

Bremer K. 1994. Branch support and tree stability. *Cladistics* **10:** 295–304.

Burk A, Douzery EJP, Springer MS. 2002. The secondary structure of mammalian mitochondrial 16S rRNA molecules: refinements based on a comparative phylogenetic approach. *Journal of Mammalian Evolution* **9:** 225–252.

Czaplewski NJ. 1997. Chiroptera. In: Kay RF, Madden RH, Cifelli RL, Flynn JJ, eds. *Vertebrate paleontology in the neotropics: the Miocene fauna of la Venta, Colombia*. Washington, DC: Smithsonian Institution Press, 410–431.

Czaplewski NJ, Cartelle C. 1998. Pleistocene bats from cave deposits in Bahia, Brazil. *Journal of Mammalogy* **79:** 784–803.

Czaplewski NJ, Morgan GS. 2003. Fossil bats of the Americas. http://www.snomnh.ou.edu/collections%26research/vertebrate_paleontology/fossil_bats/index.shtml.

Czaplewski NJ, Morgan GS, Naeher T. 2003. Molossid bats from the late Tertiary of Florida with a review of the Tertiary Molossidae of North America. *Acta Chiropterologica* **5:** 61–74.

Dávalos LM, Jansa SA. 2004. Phylogeny of the Lonchophyllini (Chiroptera: Phyllostomidae). *Journal of Mammalogy* **85:** 404–413.

Dobson GE. 1878. *Catalogue of the chiroptera in the collection of the British Museum*. London: British Museum.

Eriksson T. 1999. *AutoDecay*, 4th edn. Stockholm: Bergius Foundation, Royal Swedish Academy of Sciences.

Goldman N, Anderson JP, Rodrigo AG. 2000. Likelihood-based tests of topologies in phylogenetics. *Systematic Biology* **49:** 652–670.

Gray JE. 1838. A revision of the genera of bats (Vespertilionidae), and the description of some new genera and species. *Magazine of Zoology and Botany* **2:** 483–505.

Gray JE. 1843. [Letter addressed to the Curator]. *Proceedings of the Zoological Society of London* **1843:** 50.

Griffiths TA, Klingener D. 1988. On the distribution of Greater Antillean bats. *Biotropica* **20:** 240–251.

Gutiérrez EE. 2004. *Morfometría de los murciélagos de la familia Mormoopidae en Venezuela.* Unpublished thesis, Universidad de los Andes, Mérida.

Huelsenbeck JP, Ronquist F. 2001. MRBAYES: Bayesian inference of phylogenetic trees. *Bioinformatics* **17:** 754–755.

Kennedy M, Paterson AM, Morales JC, Parsons S, Winnington AP, Spencer HG. 1999. The long and short of it: branch lengths and the problem of placing the New Zealand short-tailed bat, *Mystacina*. *Molecular Phylogenetics and Evolution* **13:** 405–416.

Kirsch JAW, Hutcheon JM, Byrnes DGP, Lloyd BD. 1998. Affinities and historical zoogeography of the New Zealand short-tailed bat, *Mystacina tuberculata* Gray 1843, inferred from DNA-hybridization comparisons. *Journal of Mammalian Evolution* **5:** 33–64.

Koopman KF. 1955. A new subspecis of *Chilonycteris* from the West Indies and a discussion of the mammals of La Gonave. *Journal of Mammalogy* **36:** 109–113.

Koopman K. 1994. Chiroptera: systematics. *Handbuch der Zoologie* **8:** 1–217.

Lewis Oritt N, Porter CA, Baker RJ. 2001. Molecular systematics of the family Mormoopidae (Chiroptera) based on cytochrome *b* and recombination activating gene 2 sequences. *Molecular Phylogenetics and Evolution* **20:** 426–436.

Lockhart PJ, Steel MA, Hendy MD, Penny D. 1994. Recovering evolutionary trees under a more realistic model of sequence evolution. *Molecular Biology and Evolution* **11:** 605–612.

Miller GS. 1902. Twenty new American bats. *Proceedings of the Academy of Natural Sciences of Philadelphia* **54:** 389–412.

Morgan G. 2001. Patterns of extinction in West Indian bats. In: Woods CA, Sergile FE, eds. *Biogeography of the West Indies*. Boca Raton, FL: CRC Press, 369–407.

Pierson ED, Sarich VM, Lowenstein JM, Daniel MJ, Rainey WE. 1986. A molecular link between the bats of New Zealand and South America. *Nature* **323:** 60–63.

Posada D, Crandall KA. 1998. MODELTEST: testing the model of DNA substitution. *Bioinformatics* **14:** 817–818.

Rambaut AE, Grassly NC. 1997. SEQ-GENERAL: an application for the Monte Carlo simulation of DNA sequence evolution along phylogenetic trees. *Computer Applications in the Biosciences* **13:** 235–238.

Ray CE, Olsen SJ, Gut HJ. 1963. Three mammals new to the Pleistocene fauna of Florida, and a reconsideration of five earlier records. *Journal of Mammalogy* **44:** 373–395.

Ronquist F. 1997. Dispersal-vicariance analysis: a new approach to the quantification of historical biogeography. *Systematic Biology* **46:** 195–203.

Shimodaira H, Hasegawa M. 1999. Multiple comparisons of log-likelihoods with applications to phylogenetic inference. *Molecular Biology and Evolution* **16:** 1114–1116.

Silva-Taboada G. 1974. Fossil Chiroptera from cave deposits in central Cuba, with description of two new species (Genera *Pteronotus* and *Mormoops*) and the first West Indian record of *Mormoops megalophylla*. *Acta Zoologica Cracoviensia* **19:** 33–73.

Simmons NB. 2005. Order Chiroptera. In: Wilson DE, Reeder DM, eds. *Mammal species of the world: a taxonomic and geographyraphic reference*, 3rd edn. Baltimore, MD: Johns. Hopkins University Press.

Simmons NB, Conway TM. 2001. Phylogenetic relationships of mormoopid bats (Chiroptera: Mormoopidae) based on morphological data. *Bulletin of the American Museum of Natural History* **258:** 1–97.

Simmons NB, Voss RS. 1998. The mammals of Paracou, French Guiana: a neotropical lowland rainforest fauna part – 1. Bats. *Bulletin of the American Museum of Natural History* **237:** 1–219.

Smith JD. 1972. Systematics of the Chiropteran family Mormoopidae. *University of Kansas Museum of Natural History Miscellaneous Publication* **56:** 1–132.

Smith JD. 1976. Chiropteran evolution. In: Baker RJ, Jones JK Jr, Carter DC, eds. *Biology of the bats of the New World family Phyllostomatidae, Part I*, 49–69.

Springer MS, Douzery EJP. 1996. Secondary structure and

patterns of evolution among mammalian mitochondrial 12S rRNA molecules. *Journal of Molecular Evolution* **43:** 357–573.

Swofford DL. 2002. *PAUP*. Phylogenetic Analysis Using Parsimony (*and Other Methods)*, Version 4.0b10. Sunderland, MA: Sinauer Associates.

Swofford DL, Olsen GJ, Waddell PJ, Hillis DM. 1996. Phylogenetic inference. In: Hillis DM, Moritz C, Mable BK, eds. *Molecular systematics*, 2 edn. Sunderland, MA: Sinauer, 407–514.

Teeling EC, Madsen O, Murphy WJ, Springer MS, O'Brien SJ. 2003. Nuclear gene sequences confirm an ancient link between New Zealand's short-tailed bat and South American noctilionoid bats. *Molecular Phylogenetics and Evolution* **28:** 308–319.

Teeling EC, Springer MS, Madsen O, Bates P, O'Brien SJ, Murphy WJ. 2005. A molecular phylogeny for bats illuminates biogeography and the fossil record. *Science* **307:** 580–584.

Templeton AR. 1983. Phylogenetic inference from restriction endonuclease cleavage site maps with particular reference to the evolution of humans and apes. *Evolution* **37:** 221–244.

Thomas O. 1892. Note on Mexican examples of *Chilonycteris davyi*, Gray. *Annals and Magazine of Natural History, Series* **6:** 410.

Thompson JD, Higgins DG, Gibson TJ. 1994. CLUSTAL W: improving the sensitivity of progressive multiple sequence alignment through sequence weighting, position-specific gap penalties, and weight matrix choice. *Nucleic Acid Research* **22:** 4673–4680.

Van Den Bussche RA, Hoofer SR. 2000. Further evidence for inclusion of the New Zealand short-tailed bat (*Mystacina tuberculata*) within Noctilionoidea. *Journal of Mammalogy* **81:** 865–874.

Van Den Bussche RA, Hoofer SR. 2001. Evaluating the monophyly of Nataloidea (Chiroptera) with mitochondrial DNA sequences. *Journal of Mammalogy* **82:** 320–327.

Van Den Bussche RA, Weyandt AE. 2003. Mitochondrial and nuclear DNA sequence data provide resolution to sister-group relationships within *Pteronotus* (Chiroptera: Mormoopidae). *Acta Chiropterologica* **5:** 1–13.

Van Den Bussche RA, Hoofer SR, Hansen EW. 2002a. Characterization and phylogenetic utility of the mammalian protamine P1 gene. *Molecular Phylogenetics and Evolution* **22:** 333–341.

Van Den Bussche RA, Hoofer SR, Simmons NB. 2002b. Phylogenetic relationships of mormoopid bats using mitochondrial gene sequences and morphology. *Journal of Mammalogy* **83:** 40–48.

Van Den Bussche RA, Reeder SA, Hansen EW, Hoofer SR. 2003. Utility of the dentin matrix protein 1 (DMP1) gene for resolving mammalian intraordinal phylogenetic relationships. *Molecular Phylogenetics and Evolution* **26:** 89–101.

Wagner JA. 1843. Diagnosen neuer Arten brasilischer Handflünger. *Archiv für Naturgeschichte* **9:** 365–368.

Wetterer AL, Rockman MV, Simmons NB. 2000. Phylogeny of phyllostomid bats (Mammalia: Chiroptera): data from diverse morphological systems, sex chromosomes, and restriction sites. *Bulletin of the American Museum of Natural History* **248:** 1–200.

APPENDIX

Taxa, localities, tissue vouchers and GenBank accession number for sequences used in this study

Taxon	Locality	Country	Tissue voucher	Sequences
Saccopteryx bilineata				AF044664
Saccopteryx bilineata			AMNH267842	AF263213 mtrDNA AY141015 *Rag2*
Mystacina tuberculata	Little Barrier Island	New Zealand		AF144068
Mystacina tuberculata		New Zealand	UWZM-M27027	AF263222 mtrDNA AY141021 *Rag2*
Noctilio leporinus	0.5 km E Confer, Chemin, St George	Grenada	TK18513	AF330796
Noctilio leporinus			TK18515	AF263224 mtrDNA
Noctilio leporinus	Craigston estate, Carriacou Island	Grenada	TK18701	AF316477 *Rag2*
Noctilio albiventris	5840.99N, 57851.529W, 41 m elevation, Dubulay Ranch, Berbice District	Guyana	TK86633	AF330803, AF330810 *Rag2*
Noctilio albiventris			TK46004	AF263223 mtrDNA
Artibeus jamaicensis		Puerto Rico		AF061340 mtDNA
Artibeus jamaicensis				AY011963 *Rag2*
Pteronotus parnellii	24 km W St Ann's Bay, St Ann's Parish	Jamaica	TK27704	AF338661
Pteronotus parnellii	St Clair Cave, Polly Ground, St Catherine	Jamaica	AMCC102714	AY604456
Pteronotus pusillus	La Entrada (de Cabrera), Mar'a Trinidad Sánchez	Dominican Republic	AMCC103048	AY604455
Pteronotus pusillus	La Entrada (de Cabrera), Mar'a Trinidad Sánchez	Dominican Republic	AMCC103050	AY604454
Pteronotus portoricensis	Caribbean National Forest, Naguabo	Puerto Rico	TK21800	AF338665
Pteronotus portoricensis	Caribbean National Forest, Naguabo	Puerto Rico	TK21806	AF338666
Pteronotus rubiginosus	25 miles W Ciudad Valles, San Luis Potosi	Mexico	TK14517	AF338663
Pteronotus rubiginosus	19°19.19N, 100°27.89W Benito Juarez, Cerro Colorado 1350 m, Durango	Mexico	TK45500	AF338667, AF407181 mtrDNA
Pteronotus rubiginosus	Rio de Atoyac, Ojo de Agua, 14 km N 22 km E Cordoba, Veracruz	Mexico	TK13108	AF338664
Pteronotus rubiginosus	8.5 miles SSW San Lorenzo, Valle	Honduras	TK40197	AF338662
Pteronotus rubiginosus	7°22.179N, 50°29.459W, 142.0 m elev. Baramita, NW District	Guyana	TK86526	AF338668
Pteronotus '*rubiginosus*'	Oelemarie, Marowijn	Suriname	TK17953	AF330807, AF407180 mtrDNA, AF330817 *Rag2*
Pteronotus '*rubiginosus*'	Near Sinnamary, Paracou, Cayenne	French Guiana	AMCC110395	AY604457, AF263221 mtrDNA, AY245416 *Rag2*
Pteronotus psilotis	Tehuantepec, Oaxaca	Mexico	TK12043	AF338680, AF407182 mtrDNA, AF338699 *Rag2*
Pteronotus psilotis	Grutas de Lanquin, Alta Verpaz [sic]	Guatemala	CN98438	AF338677, AF338697 *Rag2*
Pteronotus personatus	0.5 km E El Manteco, Bolivar	Venezuela	TK19079	AF338678

APPENDIX *Continued*

Taxon	Locality	Country	Tissue voucher	Sequences
Pteronotus personatus	Karanambo, Upper Takutu	Guyana	CN97943	AF338676, AF338698 *Rag2*
Pteronotus 'personatus'	Grassalco, Nickerie	Suriname	TK10336	AF338679
Pteronotus davyi	1 mile above mouth of Layou River, St Joseph Parish	Dominica	TK15571	AF338669
Pteronotus davyi			TK155751 [sic]	AF407175 mtrDNA
Pteronotus davyi	3 mile S 3.0 mile W Cumuto, Arena Reserve, Nariva	Trinidad	TK25127	AF338671, AF407176 mtrDNA, AF338692 *Rag2*
Pteronotus fulvus	Chamela, Jalisco	Mexico	TK27642	AF338672, AF338693 *Rag2*
Pteronotus fulvus	El Refugio, El Imposible, Ahuachapan	El Salvador	CN101305	AF338670, AF338691 *Rag2*
Pteronotus gymnonotus	Parque Nacional Altos de Campana, Panama	Panama	CN104265	AF338673, AF338694 *Rag2*
Pteronotus gymnonotus	35 km ESE of Caicara, Hato La Florida, Bolivar	Venezuela	CN107925	AF338675
Pteronotus gymnonotus	1 km S Tingo Maria, Leoncia Prado, Huanuco Department	Peru	TK22845	AF338674, AF407177 mtrDNA
Pteronotus macleayii	Guantanamo Bay Naval Station, Guantanamo Province	Cuba	TK32162	AF338700, AF407178 mtrDNA, AF338700 *Rag2*
Pteronotus macleayii	St Clair Cave, St Catherine Parish	Jamaica	TK11008	AF338684
Pteronotus macleayii	St Clair Cave, Polly Ground, St Catherine	Jamaica	AMCC102719	AY604461
Pteronotus quadridens	Guantanamo Bay Naval Station, Guantanamo Province	Cuba	TK32171	AF338683, AF407179 mtrDNA, AF338695 *Rag2*
Pteronotus quadridens	St Clair Cave, St Catherine Parish	Jamaica	TK9487	AF338682, AF338696 *Rag2*
Pteronotus quadridens	St Clair Cave, St Catherine Parish	Jamaica	AMCC102720	AY604458
Pteronotus quadridens	La Entrada (de Cabrera), María Trinidad Sánchez	Dominican Republic	AMCC103036	AY604459
Pteronotus quadridens	Mata de Plátano, Arecibo	Puerto Rico	AMCC102335	AY604460
Mormoops blainvillei	Guantanamo Bay Naval Station, Guantanamo Province	Cuba	TK32166	AF338685, AF407172 mtrDNA, AY028169 *Rag2*
Mormoops blainvillei	Monarva Cave, Revival, Westmoreland	Jamaica	AMCC102762	AY604462
Mormoops blainvillei	St Clair Cave, St Catherine Parish,	Jamaica	TK9469	AF338686, AF338701 *Rag2*
Mormoops megalophylla	Presidio Co., Texas	United States	TK48165	AF338687, AY141020 *Rag2*
Mormoops megalophylla	Black Gap Wildlife Management Area, Brewster Co, Texas	United States	TK78661	AF263220 mtrDNA, AY141020 *Rag2*
Mormoops megalophylla	Chamela, Jalisco	Mexico	TK27640	AF330808, AF407174 mtrDNA, AF330818 *Rag2*
Mormoops megalophylla	8.2 miles S Pina [sic] Blanca, Queretaro	Mexico	TK4833	AF338689
Mormoops megalophylla	Grutas de Lanquin, Alta Verapaz	Guatemala	CN98443	AF338690, AF338702 *Rag2*
Mormoops megalophylla	7 km NW Barinitas, Barinas	Venezuela	TK19311	AF338688, AF407173 mtrDNA

For subspecies classification, see Table 1. AMCC, Ambrose Monell Cryogenic Collection of the American Museum of Natural History; AMNH, cadaver voucher at the Mammalogy Department of the American Museum of Natural History; CN, Royal Ontario Museum; TK, tissue collection of the Museum of Texas Tech University; UWZM, University of Wisconsin Zoological Museum. Sequences are cytochrome *b* unless otherwise noted.